

Original Article

Investigating Deformation and Stress Distribution in Ball Bearings Using Finite Element Analysis

Jay M. Pujara¹, Rupesh L. Patel², Jaydeep K. Dadhaniya³, Kalpesh K. Dave⁴, Hardik N. Jani⁵, Dipak R. Bhatti⁶

^{1,4,5}Department of Mechanical Engineering, Lukhdhirji Engineering College, Morbi, Gujarat, India.

^{2,3,6}Department of Mechanical Engineering, Government Engineering College, Rajkot, Gujarat, India.

¹Corresponding Author : jay.pujara42@gmail.com

Received: 18 June 2024

Revised: 26 July 2024

Accepted: 17 August 2024

Published: 31 August 2024

Abstract - This research focuses on the deformation and stress responses of five materials—Structural Steel, Chrome Steel AISI 5200, Aluminum Alloy, Brass C3700, and Cast Iron EN GJL100—under varying pressure conditions utilizing Finite Element Analysis (FEA). The study aims to provide a comprehensive understanding of how these materials behave when subjected to different levels of pressure, specifically at 50, 60, 70, 80, and 90 MPa. The results indicate that Brass C3700 consistently exhibits the highest tensile stress resistance, making it highly suitable for applications that demand superior strength and durability. Aluminum Alloy also shows significant tensile strength, performing well under increased loads, which highlights its potential for high-stress applications. Structural Steel and Chrome Steel AISI 5200 demonstrate similar performance trends, maintaining moderate stress levels and exhibiting predictable behavior under varying pressure conditions. These materials offer reliable performance and are suitable for applications where moderate stress resistance is sufficient. Cast Iron EN GJL100, while showing moderate tensile stress resistance, aligns closely with the steel materials and provides a balance of strength and predictability, making it a viable option for various industrial applications. The use of computational simulation tools, such as FEA, proves invaluable in this research. These tools enable the simulation and investigation of deformation and stress responses under various load conditions, providing detailed insights into material behavior before actual implementation. This capability allows engineers to make informed decisions regarding material selection, optimizing material usage and enhancing the reliability and safety of engineering designs. The findings from this study offer valuable guidance for material selection in industrial applications, ensuring that materials are chosen based on their performance characteristics under operational conditions.

Keywords - Finite Element Analysis (FEA), Material deformation, Stress response, Structural steel, Chrome steel AISI 5200, Aluminum alloy, Brass C3700, Cast Iron EN GJL100, Material selection.

1. Introduction

Ball bearings are ubiquitous components in a vast array of machines, underpinning smooth rotational motion and load-bearing capabilities across diverse applications. From industrial giants to high-precision aerospace systems, their reliable performance is paramount [1].

However, a persistent challenge in engineering design lies in accurately predicting the fatigue life of these bearings, which is heavily influenced by repeated cycles of stress [2].

Precise prediction is crucial for preventing unexpected failures, minimizing maintenance costs, and ensuring the safety and reliability of entire mechanical systems [3].

In recent years, Finite Element Analysis (FEA) has emerged as an influential tool for investigating the behaviour of ball bearings under various loading conditions [4].

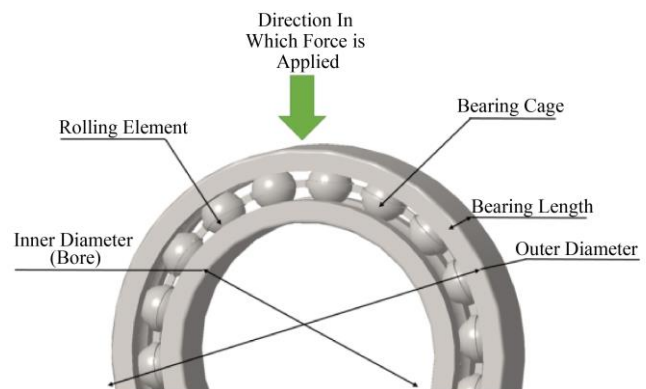


Fig. 1(a) Discretization of bearing parts F.E.A.

Figure 1(a) represents discretization of bearing parts. By simulating static, dynamic, and fatigue stresses, FEA offers invaluable insights into the deformation, stress distribution, and potential failure points within the intricate geometries of



these bearings [5, 6]. This research investigates the application of advanced FEA methodologies to predict the fatigue life of SKF ball bearings, a leading manufacturer renowned for their high-quality bearing solutions [7].

The core of this study focuses on the performance of various engineering materials traditionally employed in bearing construction, specifically exploring the behaviour of stainless steel and its alloys [1]. FEA simulations will be conducted on these materials under a range of static and dynamic loading conditions to elucidate their impact on bearing fatigue life [8, 9]. By strategically integrating FEA results with experimental data, this research aims to refine the accuracy of fatigue life predictions and pave the way for the development of more durable and efficient bearing designs [10, 11]. This research draws inspiration and methodologies from a wealth of existing literature and pioneered the application of FEA for fatigue life prediction in ball bearings, establishing a valuable foundation for further exploration [12]. The researcher provided a comprehensive review of fault modeling and predictive health monitoring techniques for rolling element bearings, offering valuable insights into potential failure mechanisms [13]. The author specifically addressed the fatigue analysis of ball bearings employed in demanding aerospace applications, highlighting the critical role of FEA in such endeavours [14]. The author emphasized the importance of advanced computational tools like FEA in predicting the fatigue life of bearing systems, underscoring the methodology's effectiveness [15]. Further explored the application of FEA in analysing the stress and fatigue behavior of ball bearings subjected to variable loading conditions, demonstrating the versatility of the technique [16]. Another researcher successfully employed FEA methods to estimate the fatigue life of roller bearings, providing valuable insights transferable to ball bearings [17]. Utilized FEA to investigate the deformation and stress distribution within bearings under dynamic loading, further solidifying the methodology's role in bearing analysis [18]. Conducted FEA simulations to analyse contact stress and fatigue life in high-speed ball bearings, highlighting the importance of considering bearing operating speeds [19]. Presented a computational approach using FEA for fatigue life prediction of wind turbine bearings, showcasing the applicability of the technique across diverse industrial sectors [20].

2. Literature Review and Gaps

The prediction of fatigue life in ball bearings using Finite Element Analysis (FEA) is a critical area of research due to its direct impact on the reliability and maintenance of mechanical systems. By simulating stress distributions under operational conditions, FEA enables engineers to anticipate potential failure points and optimize maintenance schedules. However, current studies often fall short in providing detailed analyses across a broad range of materials and loading scenarios, highlighting a gap that this research seeks to address. The refinement of FEA models to better simulate

material behaviors under varying conditions is essential for producing more accurate and universally applicable predictions.

In addition to fatigue life prediction, integrating FEA with predictive maintenance strategies is increasingly recognized as pivotal for extending the lifespan of rolling element bearings. The challenge lies in effectively combining real-time data with FEA models to allow for continuous health monitoring. Despite advancements, there remains a significant need for seamless integration of data streams to improve diagnostic accuracy and optimize maintenance. This gap underscores the importance of developing advanced predictive tools capable of real-time failure prevention, particularly in complex environments like aerospace, where precise fatigue analysis under dynamic loading conditions is crucial for ensuring safety and reliability.

2.1. Fatigue Life Prediction of Ball Bearings

The research focused on predicting the fatigue life of ball bearings using Finite Element Analysis (FEA), which aims to enhance reliability in mechanical systems. By analyzing stress distributions under operational conditions [1][11], researchers seek to provide accurate predictions crucial for maintenance planning and component lifespan optimization. However, existing studies highlight a need for more detailed analyses of stress distributions across varying materials [1][11]. This gap underscores the importance of refining FEA models to better simulate material behaviors under different loading conditions, ensuring robust predictions applicable to diverse industrial contexts.

2.2. Rolling Element Bearing Fault Modelling and Predictive Health Monitoring

Integrating FEA with predictive maintenance strategies is pivotal for prolonging the lifespan of rolling element bearings [2][12]. This research objective addresses the challenge of effectively integrating real-time data with FEA models to enable continuous health monitoring [2][12]. Current studies emphasize the necessity for seamless integration of data streams to enhance diagnostic accuracy and optimize maintenance schedules. This integration gap motivates researchers to develop advanced predictive tools that can efficiently predict and prevent bearing failures in real-time scenarios.

2.3. Fatigue Analysis of Ball Bearings in Aerospace Applications

The fatigue analysis of ball bearings in aerospace applications using FEA is critical due to the complex loading conditions involved [3][18]. This objective seeks to refine FEA models for more precise simulations of aerospace-specific loading conditions [3][18]. The existing research identifies a need for improved modeling techniques that can accurately represent the dynamic operational environments

experienced by aerospace bearings. Addressing this gap is crucial for enhancing the reliability and safety of aerospace systems through more accurate fatigue life predictions.

2.4. Advanced Computational Tools for Fatigue Life Prediction of Bearing Systems

Efforts to incorporate various loading conditions and material properties into FEA models aim to advance the accuracy of fatigue life predictions [4][24]. This objective highlights a significant gap in current research—the need for extensive validation of FEA models against experimental data [4][24]. By validating models more comprehensively, researchers can enhance the reliability of predictions and facilitate better decision-making in bearing system design and maintenance strategies.

2.5. Stress and Fatigue Analysis of Ball Bearings under Variable Loading Conditions

Investigating stress and fatigue life under variable loading conditions using FEA is crucial for understanding bearing performance in dynamic environments [5][7][8]. This objective addresses the need for more dynamic analysis techniques capable of simulating diverse variable loads [5][7][8]. Current research emphasizes the importance of capturing complex stress responses accurately to improve the

durability and efficiency of ball bearings across various industrial applications.

2.5.1. Ball Bearings and their Loading Boundary Conditions

Ball bearings are crucial components in mechanical systems, tasked with reducing friction and facilitating smooth rotational motion. Understanding their loading boundary conditions is essential both in practical applications and in Finite Element Analysis (FEA) simulations.

2.6. Research Gap and Problem Definition

While finite element analysis (FEA) has significantly advanced the prediction of ball bearing fatigue life, current studies reveal a critical need for more detailed analyses across varying materials and loading conditions. Existing models often lack the accuracy required to simulate the complex behaviors of materials under dynamic operational environments, particularly in high-stakes applications and many industrial practices. The integration of real-time data with FEA for predictive maintenance remains underexplored, limiting the ability to monitor and prevent failures continuously. This research seeks to address these gaps by refining FEA models to more accurately predict fatigue life, incorporating diverse material properties.

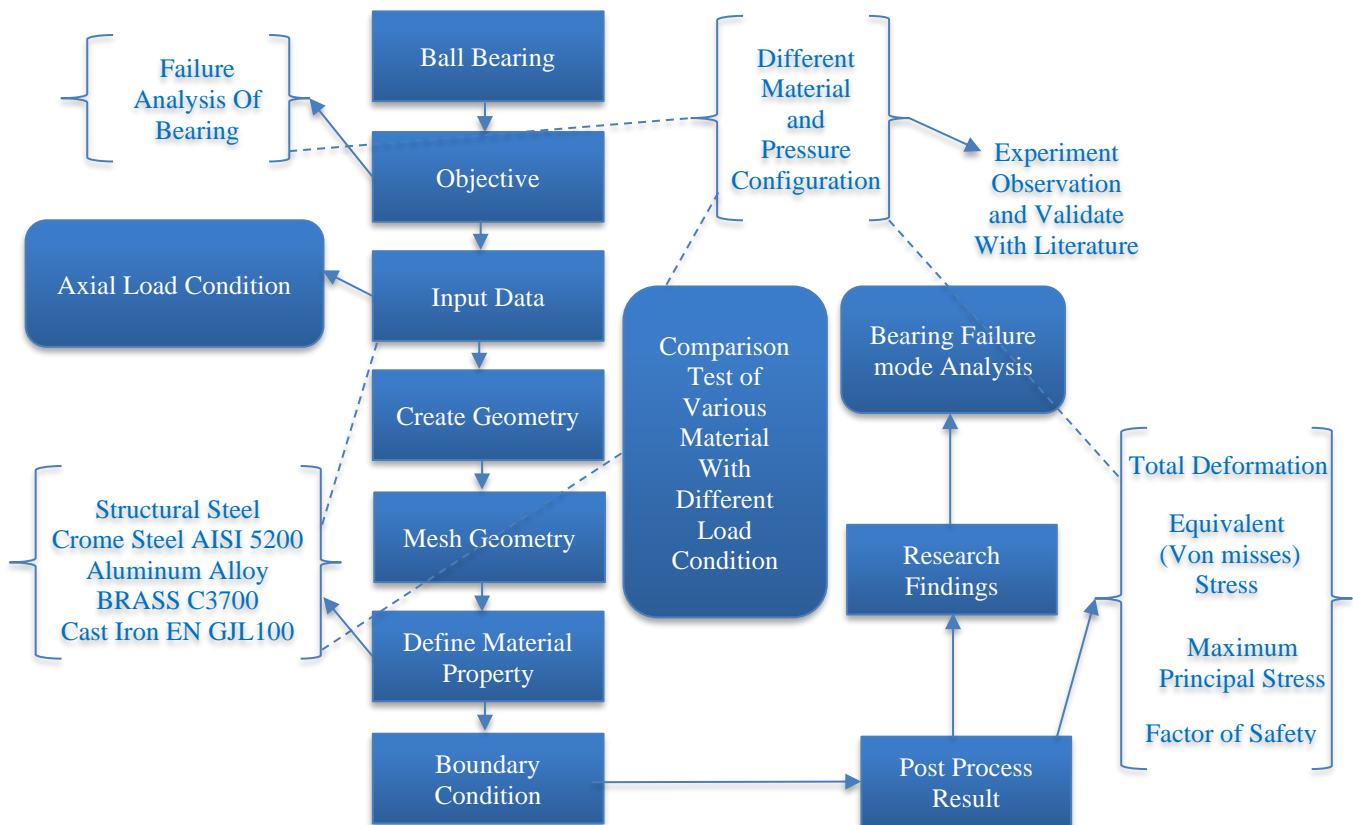


Fig. 1(b) Methodology of research study

3. Methodology and Simulation Setup

In practical applications, ball bearings experience varying loading conditions depending on their use. The primary types of loads encountered include:

- **Radial Loads:** These loads act perpendicular to the shaft's axis, exerting force from the side. Radial loads are common in applications where the bearing supports rotational shafts that carry weight or transmit force through a pulley or gear.
- **Axial Loads:** Axial loads act parallel to the shaft's axis, either pushing or pulling the shaft along its length. This type of load is prevalent in applications involving thrust or axial movements, such as in gearboxes or axial fans.
- **Combined Loads:** Bearings often experience combinations of radial and axial loads simultaneously. These conditions require bearings to handle both types of forces concurrently, affecting their fatigue life and performance.

Figure 1(b) represents the methodology of the present study.

This Research Study analyses the failure of a ball bearing under axial load conditions using Finite Element Analysis (FEA). The process begins with defining the objective, gathering input data, and selecting materials such as Structural Steel, Chrome Steel, Aluminum Alloy, Brass, and Cast Iron. The geometry is created and meshed in ANSYS, followed by defining material properties and applying boundary conditions. The model is then tested under various load and Material Property conditions, with results such as total deformation, equivalent stress, maximum principal stress, and the factor of safety being analyzed. The findings are validated through comparison with literature and experimental observations, leading to a comprehensive understanding of the bearing's failure modes and performance under different conditions.

Engineers determine loading conditions by analyzing the application's requirements, such as the weight to be supported, rotational speed, and environmental factors like vibration and shock. Understanding these loads helps in selecting the appropriate bearing type, size, and material to ensure longevity and efficiency.

3.1. FEA Perspective

In FEA, accurately modelling loading boundary conditions is critical for predicting the bearing's performance and lifespan. Key considerations in FEA simulations include:

- **Load Magnitude and Direction:** FEA models simulate the actual forces applied to the bearing, considering both static and dynamic loads over time. This enables engineers to analyze stress distributions and deformations within the bearing components.
- **Boundary Constraints:** Constraints define how the bearing interacts with its surroundings, such as the housing or shaft. These constraints influence load

distribution and affect the bearing's operational behavior under different loading scenarios.

In this research, the boundary conditions were carefully selected to accurately simulate the real-world operating conditions of ball bearings used in engineering and industrial applications. The center coordinate of the bearing was fixed to represent the mounting constraints typically encountered in practical settings. This fixation ensures that the bearing's position remains stable during the analysis, providing a realistic simulation of how the bearing would behave when subjected to operational loads. A force load of 50 MPa was applied uniformly to the bearing, reflecting the high-pressure environments that these components often endure in various mechanical systems.

3.2. Material Properties

FEA allows for the simulation of various bearing materials with different properties like elasticity, strength, and fatigue resistance. This enables engineers to optimize bearing designs for specific loading conditions and operational environments.

By accurately simulating loading boundary conditions in FEA, engineers can predict the bearing's performance metrics, such as fatigue life, deformation patterns, and stress concentrations. This predictive capability aids in design optimization, reliability assessment, and, ultimately, in enhancing the operational efficiency and durability of ball bearings in diverse applications. The materials chosen for this analysis are commonly used in engineering applications, making the findings broadly applicable to real-world scenarios. By applying general boundary conditions that mirror actual load applications, the study aims to investigate the material strength and performance of each candidate under identical conditions. This approach allows for a direct comparison of material resilience and structural integrity when subjected to the same operational stresses. Finite Element Analysis (FEA) in ANSYS Workbench is a powerful tool used to simulate and analyze the behavior of engineering structures under various conditions. Here is a structured methodology to effectively solve FEA models using ANSYS Workbench, a Computational Software tool that empowers engineers to analyze designs virtually before physical prototypes are built.

The process starts with importing the Computer Aided Design (CAD) geometry of the object. Imagine a bridge - its 3D model would be imported here. Next, engineers define the material properties, like how stiff or dense the bridge components are. Then, they create a mesh, essentially a digital net cast over the model. This mesh breaks the complex geometry down into smaller, simpler elements for calculations. The next step involves defining how the real bridge would experience forces. This could involve fixing certain parts, like the bridge's base, to represent its connection

to the ground. Engineers would then apply forces or pressures, mimicking traffic or wind loads acting on the bridge. Depending on the analysis goal, different analysis types are chosen. Static analysis simulates how the bridge behaves

under its own weight and constant traffic, while transient analysis might consider how it responds to earthquakes or sudden changes in wind direction.

Table 1. Material property

| Material (Unit) | Structural Steel | Chrome Steel AISI 5200 | Aluminum Alloy | BRASS C3700 | Cast Iron EN GJL100 |
|--------------------------------------|-------------------------|-------------------------|-------------------------|-------------------------|-------------------------|
| Property | Magnitude | | | | |
| Density (kg/m ³) | 7850 | 7810 | 2770 | 8267 | 6999 |
| Young's Modulus (GPa) | 200 | 210 | 71 | 99 | 89 |
| Thermal Expansion Coefficient (1/°C) | 16.0 × 10 ⁻⁶ | 12.0 × 10 ⁻⁶ | 23.0 × 10 ⁻⁶ | 19.0 × 10 ⁻⁶ | 12.0 × 10 ⁻⁶ |
| Poisson's Ratio | 0.3 | 0.29 | 0.33 | 0.345 | 0.26 |

Once everything is set, the computational software tool uses complex math to solve the model's behavior based on the defined settings. Finally, engineers use built-in visualization tools to analyze the results. They can see how stress is distributed throughout the bridge, how much it might bend under load, and identify any potential weak points. This information helps them refine the design before building a physical prototype, saving time and resources. Several researchers have explored the validity of mathematical models [1-3] for predicting deformation and stress in materials. Their findings indicate that these models are accurate within a specific acceptable range of error.

applications without examining Brass C3700's tensile strength.

By utilizing advanced computational tools, this study enhances the accuracy of material behavior predictions, enabling more informed design and material selection decisions. It extends the application of FEA, optimizing material use, improving safety, and reducing costs in industrial contexts.

Figures 1(c),(d) and 2(a),(b) represent that the FEA results demonstrate that structural steel performs adequately under the applied boundary conditions.

This paper acknowledges this established understanding and aims to build upon it. The research will focus on commonly used engineering materials and investigate their behavior using a computational tool called Finite Element Analysis (FEA). FEA allows us to create a digital model of the material and simulate real-world conditions to analyze how it will deform and experience stress under various loads. This approach will provide valuable insights into the performance of these materials without the need for extensive physical testing.

4. Results and Discussion

This study stands out by performing a Finite Element Analysis (FEA) across a variety of materials—Chrome Steel AISI 5200, Structural Steel, Aluminum Alloy, Brass C3700, and Cast Iron EN GJL100—under different loading conditions. Unlike prior research, which often focused on a single material, this work offers a detailed comparative analysis, highlighting key performance characteristics essential for specific applications.

While existing studies have used FEA to predict fatigue life and material behavior, they generally lack the comprehensive material comparison provided here. For example, [1] concentrated on Chrome Steel without considering other materials, and [3] focused on aerospace

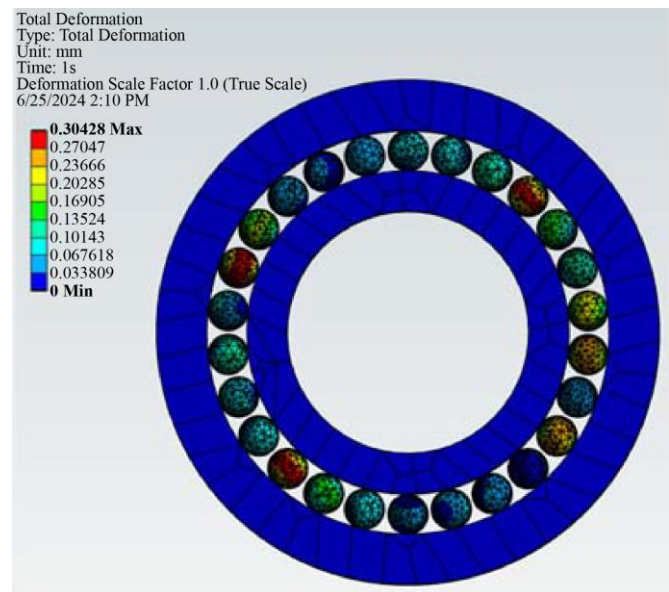


Fig. 1c) Total deformation result in F.E.A. software - Total deformation [Max. = 0.30428 mm]

With a total deformation of 0.30428 mm, equivalent stress of 937.18 MPa, and a maximum principal stress of 286.34 MPa, the material exhibits strong resistance to deformation and high stress.

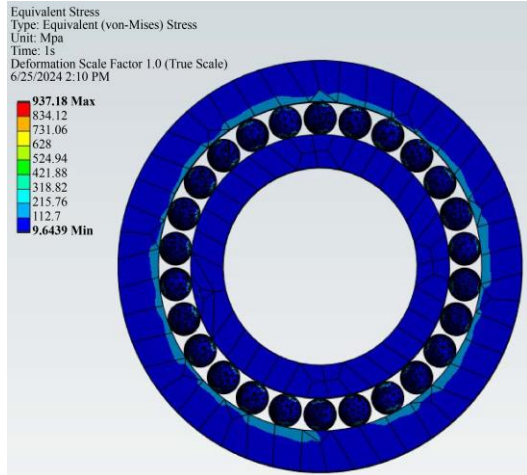


Fig. 1(d) Total deformation result in F.E.A. software - Total deformation equivalent stress [Max. = 937.18 Mpa]

total deformation of 0.28998 mm, equivalent stress of 937.54 MPa and a maximum principal stress of 283.83 MPa, the material exhibits strong resistance to deformation and high stress.

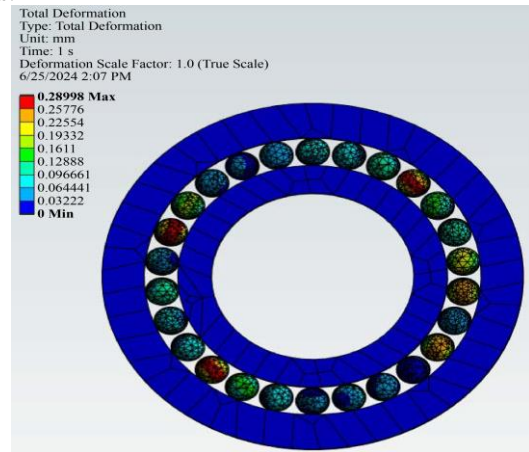


Fig. 3(a) Total deformation [Max. = 0.28998 mm]

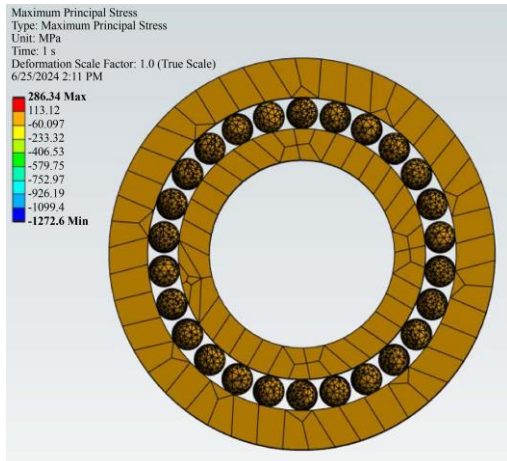


Fig. 2(a) Maximum principal stress result in F.E.A. software - [Max = 286.34 Mpa]

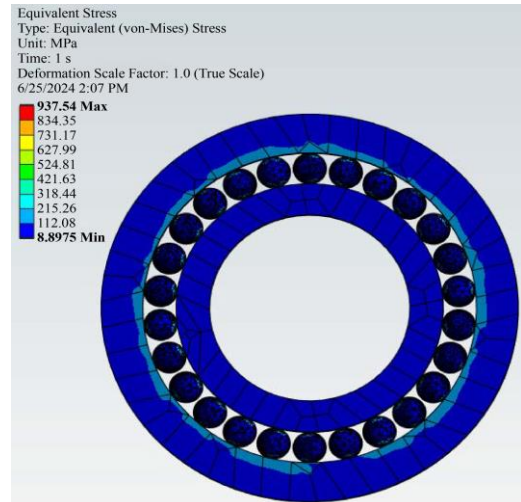


Fig. 3(b) Equivalent stress result in F.E.A. software [Max. = 937.54 Mpa]

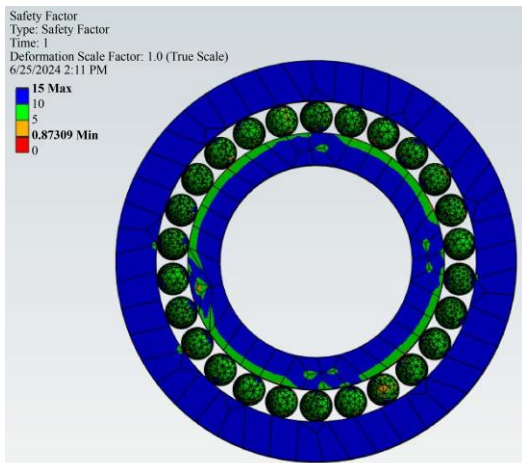


Fig. 2(b) Factor of safety result in F.E.A. software- Factor of safety [AVG = 5-8]

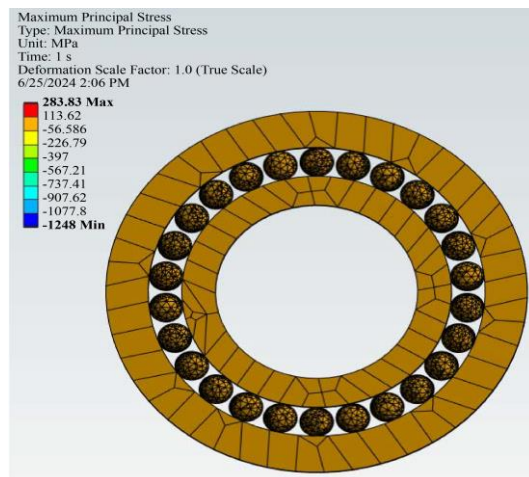


Fig. 4(a) Maximum principal stress [Max = 283.83 Mpa]

Figures 3(a),(b) and 4(a),(b) represent FEA results that demonstrate that Chrome Steel AISI 5200 performs excellently under the applied boundary conditions. With a

Figures 5 (a), (b) and 6 (a), (b) represent FEA results that demonstrate that aluminum alloy exhibits different performance characteristics under the applied boundary conditions compared to other materials.

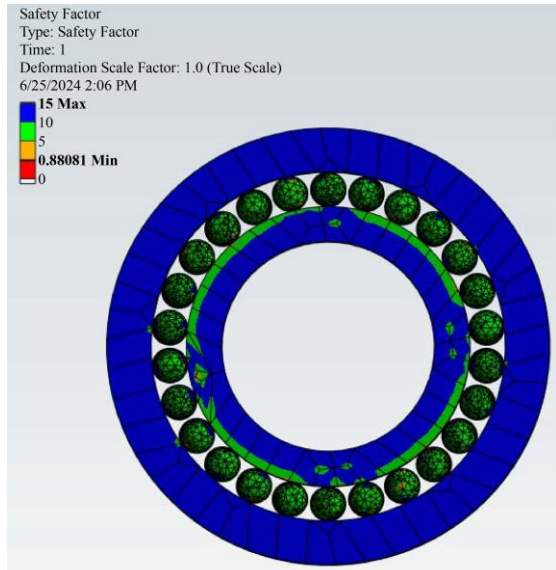


Fig. 4(b) Factor of safety result in F.E.A. software [AVG = 5-8]

With a total deformation of 0.85489 mm, equivalent stress of 936.8 MPa, and a maximum principal stress of 294.56 MPa, the material shows a higher degree of deformation but maintains strong resistance to stress.

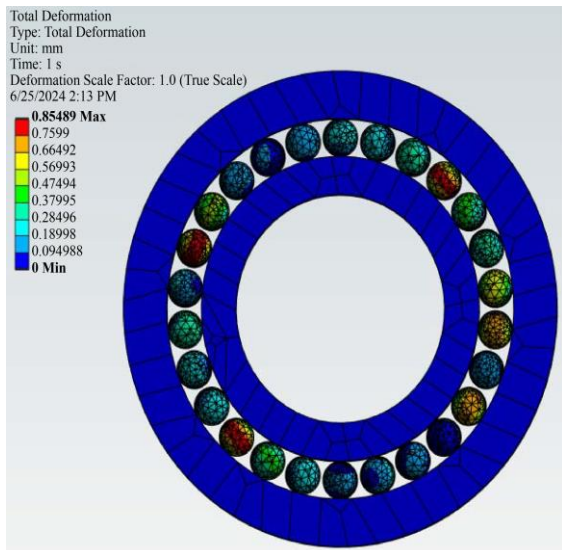


Fig. 5(a) Total deformation result in F.E.A. software [Max. = 0.85489 mm]

The safety factor ranges of 5 to 8 underscores its suitability for demanding industrial applications, providing reliable and safe performance under the specified load conditions while highlighting the need to consider its greater flexibility in design applications.

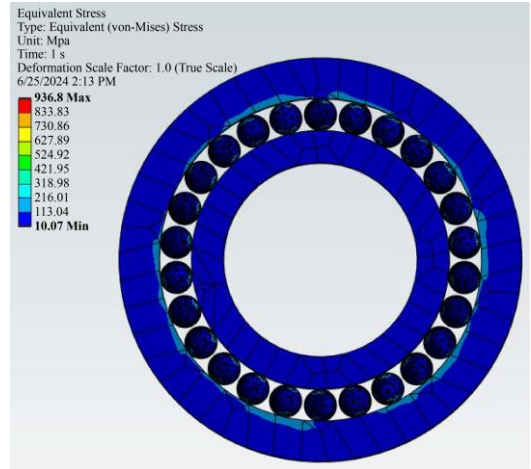


Fig. 5(b) Equivalent stress [Max. = 936.8 Mpa]

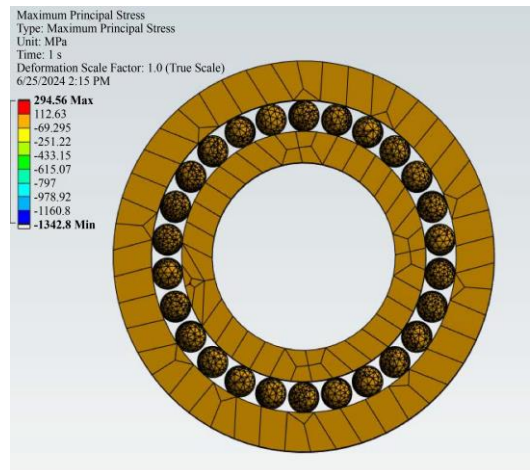


Fig. 6(a) Maximum principal stress in F.E.A. software [Max = 294.56 Mpa]

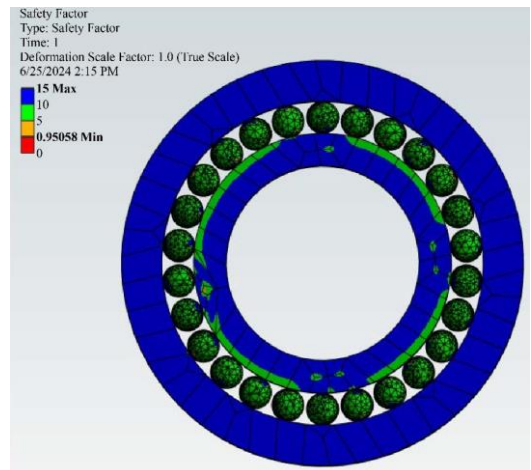


Fig. 6 (b) Factor of safety result in F.E.A. software [AVG = 5-8]

Figures 7 (a), (b) and 8 (a), (b) represent FEA results that demonstrate that Brass C3700 exhibits moderate deformation and high stress resistance under the applied boundary

conditions. With a total deformation of 0.60624 mm, equivalent stress of 936.96 MPa, and a maximum principal stress of 299.11 MPa, the material shows a good balance of flexibility and strength. The safety factor range of 1.22 to 8 underscores the need for careful application, particularly in scenarios where the lower end of the safety factor might be reached.

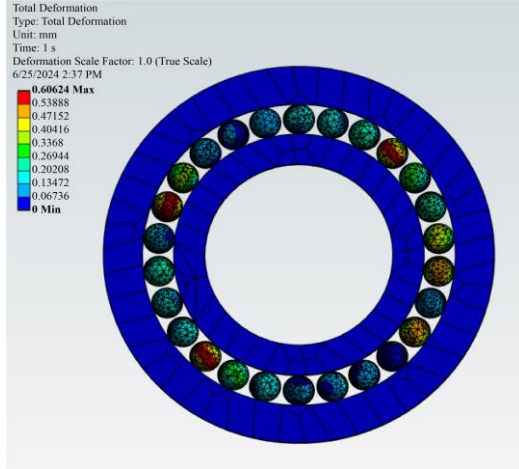


Fig. 7(a) Total deformation [Max. = 0.60624 mm]

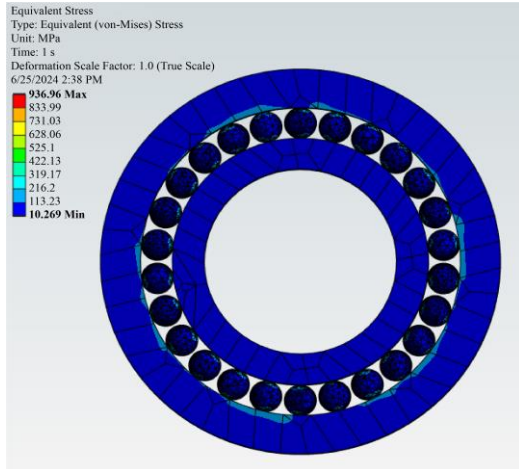


Fig. 7(b) Total deformation [Max. = 936.96 Mpa]

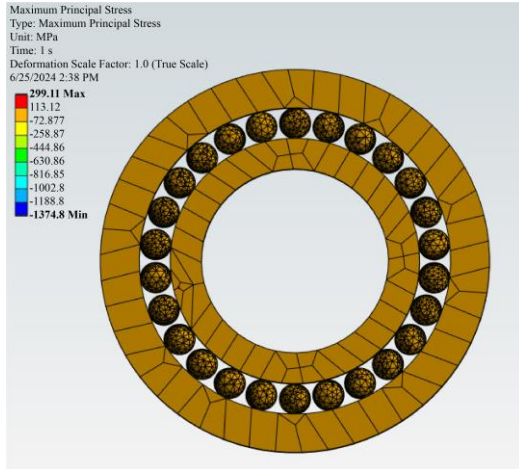


Fig. 8(a) Maximum principal stress [Max = 299.11Mpa]

Figures 9 (a), (b) and 10 (a), (b) represent FEA results. Brass C3700 remains suitable for demanding industrial applications, providing reliable performance under specified load conditions while highlighting the importance of considering its lower safety factor in critical designs. The Finite Element Analysis (FEA) results for Cast Iron EN GJL100 reveal that the material exhibits a total deformation of 0.68185 mm, an equivalent stress of 939.33 MPa, and a maximum principal stress of 276.88 MPa under the specified boundary conditions. These values indicate that Cast Iron EN GJL100 maintains moderate deformation and withstands significant internal and tensile forces. Additionally, with a safety factor ranging from 5 to 8, the material ensures a robust and reliable performance, providing a substantial margin of safety for secure operation in high-pressure industrial applications.

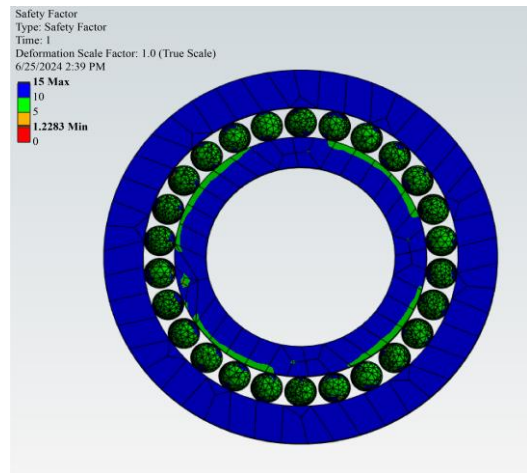


Fig. 8 (b) Factor of safety result in F.E.A. software- Factor of safety [AVG = 1.22-8]

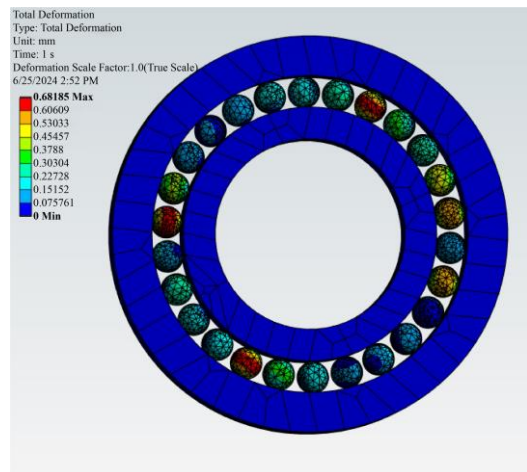


Fig. 9 (a) Total deformation [Max. = 0.68185 mm]

The Finite Element Analysis (FEA) results indicate that among the materials tested, Chrome Steel AISI 5200 and Structural Steel exhibit the lowest total deformation at 0.28998 mm and 0.30428 mm, respectively, indicating higher rigidity.

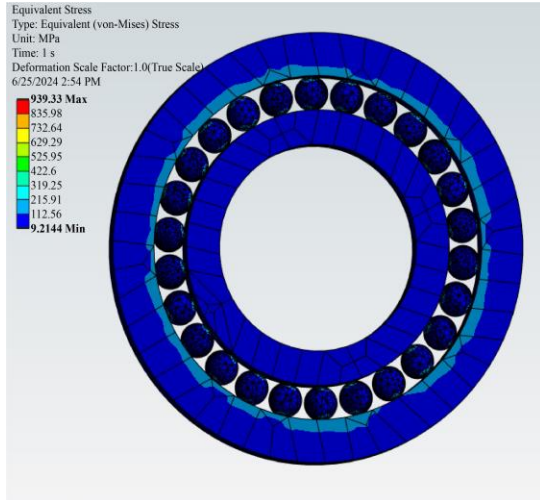


Fig. 9 (b) Equivalent Stress [Max. = 939.33 Mpa]

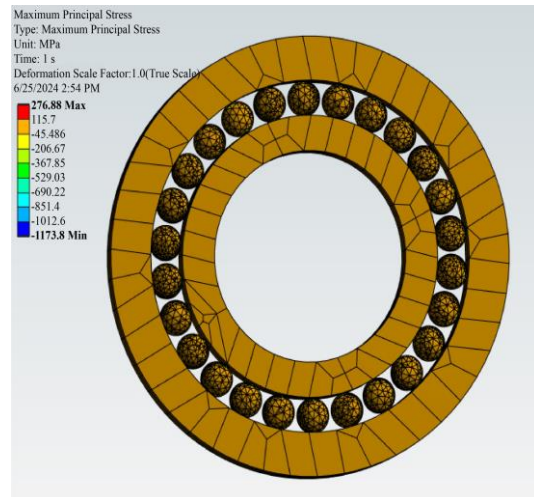


Fig. 10 (a) Maximum principal stress result in F.E.A. software [Max = 276.88Mpa]

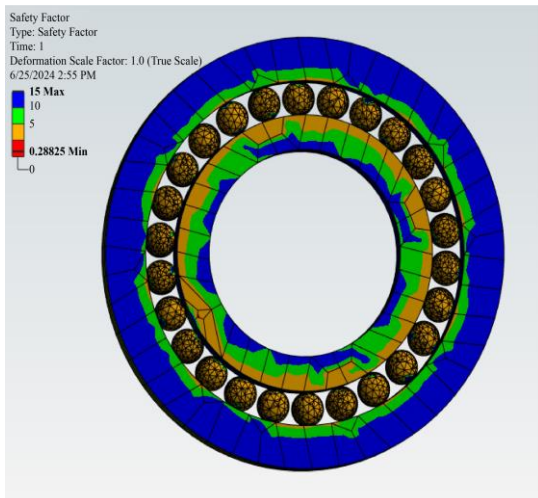


Fig. 10 (b) Factor of safety result in F.E.A. software - Factor of safety [AVG = 5-8]

All materials show similar equivalent stress levels of around 937 MPa, reflecting their comparable ability to withstand internal forces.



Fig. 11 Deformation results at various pressure magnitudes at 60Mpa,70Mpa,80Mpa, and 90 Mpa

Brass C3700 has the highest maximum principal stress at 299.11 MPa, suggesting it can endure higher tensile forces. The safety factor ranges highlight that while Structural Steel, Chrome Steel AISI 5200, and Aluminum Alloy offer robust performance with a safety factor of 5 to 8, Brass C3700's lower-end safety factor of 1.22 indicates potential vulnerability under certain conditions.

Cast Iron EN GJL100 presents moderate deformation and stress resistance, making it a reliable choice with a safety factor of 5 to 8. Overall, Chrome Steel AISI 5200 and Structural Steel emerge as the most resilient materials under the given conditions.



Fig. 12 Maximum principal stress result at various pressure magnitudes 60Mpa, 70Mpa, 80Mpa, 90 Mpa

Table 2. Result table at first run pressure = 50 Mpa

| Material | | | | | |
|---------------------------------------|-------------------------|-------------------------------|-----------------------|--------------------|----------------------------|
| Parameter | Structural Steel | Chrome Steel AISI 5200 | Aluminum Alloy | BRASS C3700 | Cast Iron EN GJL100 |
| Total Deformation (Mpa) | 0.30428 | 0.28998 | 0.85489 | 0.60624 | 0.68185 |
| Equivalent Stress (mm) | 937.18 | 937.54 | 936.8 | 936.96 | 939.33 |
| Maximum Principal Stress (Mpa) | 286.34 | 283.83 | 294.56 | 299.11 | 276.88 |

Table 3. Result table at various pressure magnitudes for structural steel

| Material Structural Steel | | | | | |
|----------------------------------|--------------------------|--------------------------|--------------------------|--------------------------|--------------------------|
| | Pressure = 50 Mpa | Pressure = 60 Mpa | Pressure = 70 Mpa | Pressure = 80 Mpa | Pressure = 90 Mpa |
| Total Deformation | 0.30428 | 0.36514 | 0.42599 | 0.48685 | 0.54771 |
| Equivalent Stress | 937.18 | 1124.6 | 1312.1 | 1499.5 | 1686.9 |
| Maximum Principal Stress | 286.34 | 283.83 | 400 | 458.14 | 515.41 |

Table 4. Result table at various pressure magnitudes for structural steel Chrome steel AISI 5200

| Chrome Steel AISI 5200 | | | | | |
|---------------------------------|--------------------------|--------------------------|--------------------------|--------------------------|--------------------------|
| Parameter | Pressure = 50 Mpa | Pressure = 60 Mpa | Pressure = 70 Mpa | Pressure = 80 Mpa | Pressure = 90 Mpa |
| Total Deformation | 0.28998 | 0.25776 | 0.34798 | 0.40598 | 0.41242 |
| Equivalent Stress | 937.54 | 937.54 | 1125 | 1312.6 | 1500.1 |
| Maximum Principal Stress | 283.83 | 340.59 | 397.36 | 454.13 | 510.89 |

Table 5. Result table at various pressure magnitudes for Chrome steel AISI 5200

| Aluminum Alloy | | | | | |
|---------------------------------|--------------------------|--------------------------|--------------------------|--------------------------|--------------------------|
| Parameter | Pressure = 50 Mpa | Pressure = 60 Mpa | Pressure = 70 Mpa | Pressure = 80 Mpa | Pressure = 90 Mpa |
| Total Deformation | 0.85489 | 1.0259 | 1.1968 | 1.3678 | 1.5388 |
| Equivalent Stress | 936.8 | 11242 | 1311.5 | 1498.9 | 1686.2 |
| Maximum Principal Stress | 294.56 | 353.47 | 412.38 | 471.29 | 530.2 |

To gain a deeper understanding of how varying pressure affects the total deformation magnitude, further investigation is essential to conduct, which is represented in Figures 11 and 12, which represent FEA results series of Finite Element Analyses (FEA) under different pressure loads of 50, 60, 70, 80, and 90 MPa, this can observe and quantify the deformation behavior of each material. This approach will help identify the pressure thresholds at which materials like Structural Steel, Chrome Steel AISI 5200, Aluminum Alloy, Brass C3700, and Cast Iron EN GJL100 begin to exhibit significant deformation changes. Analyzing these variations will provide insights into the structural integrity and performance limits of these materials under diverse operational conditions, aiding in the selection of the most

suitable material for applications requiring specific deformation tolerances.

Tables 3, 4, 5, 6 and 7 represent the data analysis of deformation and maximum principal stress for various materials under different pressure magnitudes using Finite Element Analysis (FEA) software. The pressure magnitudes examined were 60 MPa, 70 MPa, 80 MPa, and 90 MPa. The materials tested included Structural Steel, Chrome Steel AISI 5200, Aluminum Alloy, Brass C3700, and Cast Iron EN GJL100. Here, the results for Structural Steel are presented as contour plots generated by the FEA software, which provide a visual representation of the deformation and stress distribution within the material under the specified pressures.

Table 6. Result table at various pressure magnitudes for BRASS C3700

| BRASS C3700 | | | | | |
|--------------------------|-------------------|-------------------|-------------------|-------------------|-------------------|
| Parameter | Pressure = 50 Mpa | Pressure = 60 Mpa | Pressure = 70 Mpa | Pressure = 80 Mpa | Pressure = 90 Mpa |
| Total Deformation | 0.60624 | 0.72749 | 0.84873 | 0.96998 | 1.0912 |
| Equivalent Stress | 936.96 | 1124.4 | 1311.7 | 1499.1 | 1686.5 |
| Maximum Principal Stress | 299.11 | 358.93 | 418.75 | 478.58 | 538.4 |

Table 7. Result table at various pressure magnitudes for cast iron EN GJL100

| Cast Iron EN GJL100 | | | | | |
|--------------------------|-------------------|-------------------|-------------------|-------------------|-------------------|
| Parameter | Pressure = 50 Mpa | Pressure = 60 Mpa | Pressure = 70 Mpa | Pressure = 80 Mpa | Pressure = 90 Mpa |
| Total Deformation | 0.68185 | 0.81822 | 0.95459 | 1.091 | 1.2273 |
| Equivalent Stress | 939.33 | 1127.2 | 1315.1 | 1502.9 | 1690.8 |
| Maximum Principal Stress | 276.88 | 332.25 | 387.63 | 443.01 | 498.38 |

In Figure 13, the graph depicts the relationship between pressure and total deformation for various materials. The pressure is represented on the x-axis in Mega-Pascal (MPa), and the total deformation is on the y-axis in millimeters (mm) [1]. The four materials shown are structural steel, chrome steel AISI 5200, cast iron EN GJL 100, and brass C3700. It can be observed that structural steel exhibits the least amount of deformation at all pressure levels compared to the other materials. This indicates superior resistance to bending or warping under pressure. Conversely, brass C3700 shows the greatest deformation at all pressure levels [1].

This suggests that brass C3700 is less resistant to bending or warping under pressure compared to the other materials included in the graph. It is important to note that the graph only shows the behavior of these materials up to 90 MPa. How these materials deform at higher pressures is not shown in the graph.

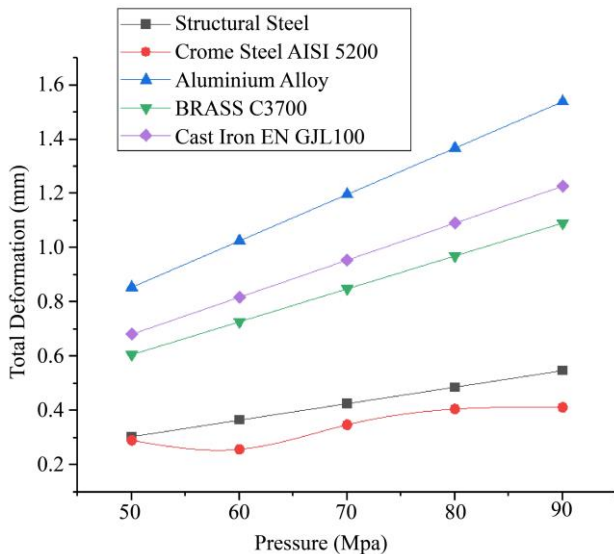


Fig. 13 Total deformation vs pressure

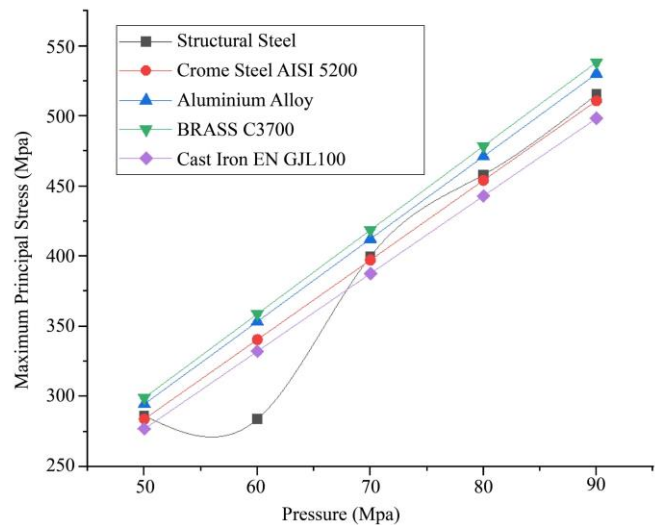


Fig. 14 Maximum principal Stress Vs pressure

In Figure 14, the graph presented illustrates the relationship between maximum principal stress (in MPa) and applied pressure (in MPa) for five different materials: Structural Steel, Chrome Steel AISI 5200, Aluminum Alloy, Brass C3700, and Cast Iron EN GJL100. As the applied pressure increases from 50 MPa to 90 MPa, all materials show a consistent rise in maximum principal stress, indicating a direct correlation between pressure and stress. Structural Steel exhibits a non-linear increase, with a deviation at 60 MPa before returning to a linear trend. Its maximum principal stress ranges from approximately 285 MPa at 50 MPa to around 480 MPa at 90 MPa.

Chrome Steel AISI 5200 shows a steady linear increase, maintaining relatively lower stress values compared to other materials except for Structural Steel, with stress ranging from around 280 MPa to about 470 MPa. Aluminum Alloy shows a higher stress increase rate, with values starting at around 295

MPa and reaching approximately 510 MPa. Brass C3700 displays the highest maximum principal stress values, starting at about 300 MPa and climbing to around 530 MPa. Cast Iron EN GJL100 exhibits a linear increase similar to Chrome Steel, with stress values ranging from around 275 MPa to about 480 MPa.

The material performance analysis reveals that Brass C3700 consistently exhibits the highest maximum principal stress values across all pressure levels, indicating its superior tensile stress resistance. Aluminum Alloy also demonstrates significant stress values, highlighting its capability to withstand high tensile forces. Structural Steel and Chrome Steel AISI 5200 show similar performance, with Structural Steel displaying a slight deviation at 60 MPa. Cast Iron EN GJL100, while exhibiting lower maximum principal stress values compared to Brass C3700 and Aluminum Alloy, aligns closely with the steel materials, reflecting moderate tensile stress resistance. This comparative analysis aids in material selection for specific engineering and industrial applications, emphasizing Brass C3700 and Aluminum Alloy for high-strength requirements and steel materials for applications with moderate stress resistance and predictable performance.

5. Conclusion

- According to the outcomes of the Finite Element Analysis (FEA), the materials that were examined show that the most stiff are Chrome Steel AISI 5200 and Structural Steel, which show the lowest total deformation at 0.28998 mm and 0.30428 mm, respectively. Comparable equivalent stress levels of approximately 937 MPa are displayed by all materials, indicating a similar capacity for withstanding internal stresses. With a maximum main stress of 299.11 MPa, brass C3700 has the greatest and may withstand higher tensile stresses. The safety factor ranges show that, whereas Brass C3700's lower-end safety factor of 1.22 suggests potential vulnerability beneath certain circumstances, Structural Steel, Chrome Steel AISI 5200, and Aluminum Alloy give strong performance with a security factor of 5 to 8. Cast Iron EN GJL100 is a dependable material because to its modest deformation and stress resistance indicating that it is a dependable option with a 5 to 8 safety factor. Overall, Chrome Steel AISI 5200 and Structural Steel emerge as

the most resilient materials under the given conditions. The finite element analysis of various materials, including Structural Steel, Chrome Steel AISI 5200, Aluminum Alloy, Brass C3700, and Cast Iron EN GJL100, under different pressure conditions reveals distinct performance characteristics. All materials show an increase in maximum principal stress with rising pressure, indicating a direct correlation between applied load and stress. Brass C3700 stands out with the highest tensile stress resistance across all pressure levels, making it highly suitable for applications requiring superior strength. Aluminum Alloy also demonstrates significant tensile strength, performing well under increased loads. Structural Steel and Chrome Steel AISI 5200 exhibit similar and reliable performance trends, maintaining moderate stress levels and showing predictable behavior under pressure. Cast Iron EN GJL100, while exhibiting moderate tensile stress resistance, aligns closely with the steel materials, offering a balance of strength and predictability.

- This comparative analysis underscores the importance of material selection based on specific application requirements. Brass C3700 and Aluminum Alloy are ideal for high-strength applications, while steel materials are suitable for scenarios where moderate stress resistance and predictable performance are desired. The insights gained from this analysis provide valuable guidance for engineering and industrial applications, ensuring the selection of materials that best meet the operational demands and safety requirements.
- The use of computational simulation tools, such as finite element analysis, proves to be invaluable in this context. These tools allow for the simulation and investigation of deformation under various load conditions, providing detailed insights into material behavior before actual implementation. By accurately predicting how different materials will react to specific stresses, engineers can make informed decisions in selecting the most appropriate materials for industrial applications. This capability not only enhances the reliability and safety of engineering designs but also optimizes material usage, contributing to more efficient and cost-effective solutions in industrial contexts.

References

- [1] Agnieszka Chudzik, and Bogdan Warda, "Fatigue Life Prediction of a Radial Cylindrical Roller Bearing Subjected to a Combined Load Using FEM," *Eksploracja i Niezawodność -Maintenance and Reliability*, vol. 22, no. 2, pp. 212-220, 2020. [[CrossRef](#)] [[Google Scholar](#)] [[Publisher Link](#)]
- [2] Idriss El-Thalji, and Erkki Jantunen, "A Summary of Fault Modelling and Predictive Health Monitoring of Rolling Element Bearings," *Mechanical Systems and Signal Processing*, vol. 60-61, pp. 252-272, 2015. [[CrossRef](#)] [[Google Scholar](#)] [[Publisher Link](#)]
- [3] Neeraj Kumar, and RK Satapathy, "Bearings in Aerospace, Application, Distress, and Life: A Review," *Journal of Failure Analysis and Prevention*, vol. 23, pp. 915-947, 2023. [[CrossRef](#)] [[Google Scholar](#)] [[Publisher Link](#)]
- [4] E. Santecchia et al., "A Review on Fatigue Life Prediction Methods for Metals," *Advances in Materials Science and Engineering*, vol. 2016, no. 1, pp. 1-26, 2016. [[CrossRef](#)] [[Google Scholar](#)] [[Publisher Link](#)]

- [5] Hongchuan Cheng et al., "Fatigue Life and Fatigue Reliability Mechanism of Ball Bearings," *Journal of Mechanics*, vol. 40, pp. 79-92, 2024. [[CrossRef](#)] [[Google Scholar](#)] [[Publisher Link](#)]
- [6] Paweł J. Romanowicz, and Bogdan Szybiński, "Fatigue Life Assessment of Rolling Bearings Made From AISI 52100 Bearing Steel," *Materials*, vol. 12, no. 3, pp. 1-23, 2019. [[CrossRef](#)] [[Google Scholar](#)] [[Publisher Link](#)]
- [7] Yi-Cheng Chen, and Chung-Biau Tsay, "Stress Analysis of a Helical Gear Set with Localized Bearing Contact," *Finite Elements in Analysis and Design*, vol. 38, no. 8, pp. 707-723, 2002. [[CrossRef](#)] [[Google Scholar](#)] [[Publisher Link](#)]
- [8] Haobo Wang, Hangyuan Lv, and Zhong Luo, "Analysis of Mechanical Properties and Fatigue Life of Microturbine Angular Contact Ball Bearings Under Eccentric Load Conditions," *Sensors*, vol. 23, no. 9, pp. 1-15, 2023. [[CrossRef](#)] [[Google Scholar](#)] [[Publisher Link](#)]
- [9] L. Reis, B. Li, and M. de Freitas, "A Multiaxial Fatigue Approach to Rolling Contact Fatigue in Railways," *International Journal of Fatigue*, vol. 67, pp. 191-202, 2014. [[CrossRef](#)] [[Google Scholar](#)] [[Publisher Link](#)]
- [10] John A. R. Bomidi et al., "Experimental and Numerical Investigation of Torsion Fatigue of Bearing Steel," *Journal of Tribology*, vol. 135, no. 3, 2013. [[CrossRef](#)] [[Google Scholar](#)] [[Publisher Link](#)]
- [11] Anil Kumar et al., "A Comprehensive Study on Developing an Intelligent Framework for Identification and Quantitative Evaluation of the Bearing Defect Size," *Reliability Engineering & System Safety*, vol. 242, 2024. [[CrossRef](#)] [[Google Scholar](#)] [[Publisher Link](#)]
- [12] S Li, C Wei, and Y Wang, "Fabrication and Service of All-ceramic Ball Bearings for Extreme Conditions Applications," *IOP Conference Series: Materials Science and Engineering*, Brasov, Romania, vol. 1009, pp. 1-10, 2021. [[CrossRef](#)] [[Google Scholar](#)] [[Publisher Link](#)]
- [13] Sudipta Saha, and M. Nabi, "Finite Element Modelling and Analysis of Axial Active Magnetic Bearing," *2018 IEEE 13th International Conference on Industrial and Information Systems (ICIIS)*, pp. 432-435, 2018. [[CrossRef](#)] [[Google Scholar](#)] [[Publisher Link](#)]
- [14] K.-D. Bouzakis, N. Vidakis, and S. Mitsi, "Fatigue Prediction of Thin Hard Coatings on the Steel Races of Hybrid Bearings Used in High-speed Machine Tool Spindles," *Journal of Tribology*, vol. 120, no. 4, pp. 835-842, 1998. [[CrossRef](#)] [[Google Scholar](#)] [[Publisher Link](#)]
- [15] Haobo Wang, Hangyuan Lv, and ZhongLuo, "Analysis of Mechanical Properties and Fatigue Life of Microturbine Angular Contact Ball Bearings Under Eccentric Load Conditions," *Sensors*, vol. 23, no. 9, pp. 1-15, 2023. [[CrossRef](#)] [[Google Scholar](#)] [[Publisher Link](#)]
- [16] Sigmund Kyrre Ås, Bjørn Skallerud, and Bård Wathne Tveiten, "Surface Roughness Characterization for Fatigue Life Predictions Using Finite Element Analysis," *International Journal of Fatigue*, vol. 30, no. 12, pp. 2200-2209, 2008. [[CrossRef](#)] [[Google Scholar](#)] [[Publisher Link](#)]
- [17] Attilio Arcari et al., "Variable Amplitude Fatigue Life in VHCF and Probabilistic Life Predictions," *Procedia Engineering*, vol. 114, pp. 574-582, 2015. [[CrossRef](#)] [[Google Scholar](#)] [[Publisher Link](#)]
- [18] Shinya Matsuda et al., "Cyclic Fatigue Life Characteristics of Ceramic Balls Under Variable Thermal Shock Loadings," *Engineering Fracture Mechanics*, vol. 255, 2021. [[CrossRef](#)] [[Google Scholar](#)] [[Publisher Link](#)]
- [19] Renshui Cao et al., "Mixed Lubrication Analysis of Tapered Roller Bearings and Crowning Profile Optimization Based on Numerical Running-in Method," *Lubricants*, vol. 11, no. 3, pp. 1-20, 2023. [[CrossRef](#)] [[Google Scholar](#)] [[Publisher Link](#)]
- [20] Steven J. Lorenz et al., "Investigation into Rolling Contact Fatigue Performance of Aerospace Bearing Steels," *International Journal of Fatigue*, vol. 172, 2023. [[CrossRef](#)] [[Google Scholar](#)] [[Publisher Link](#)]
- [21] Jae-Il Hwang, and Gerhard Poll, "A New Approach for the Prediction of Fatigue Life in Rolling Bearings Based on Damage Accumulation Theory Considering Residual Stresses," *Frontiers in Manufacturing Technology*, vol. 2, 2022. [[CrossRef](#)] [[Google Scholar](#)] [[Publisher Link](#)]
- [22] M.Y. Toumi et al., "Numerical Simulation and Experimental Comparison of Flaw Evolution on a Bearing Raceway: Case of Thrust Ball Bearing," *Journal of Computational Design and Engineering*, vol. 5 no. 4, pp. 427-434, 2018. [[CrossRef](#)] [[Google Scholar](#)] [[Publisher Link](#)]
- [23] Mian Hammad Nazir, Zulfiqar Ahmad Khan, and Adil Saeed "Experimental Analysis and Modelling of C-crack Propagation in Silicon Nitride Ball Bearing Element Under Rolling Contact Fatigue," *Tribology International*, vol. 26, pp. 386-401, 2018. [[CrossRef](#)] [[Google Scholar](#)] [[Publisher Link](#)]
- [24] Shirmendagva Darisuren et al., "A Study on the Improvement of the Fatigue Life of Bearings by Ultrasonic Nanocrystal Surface Modification Technology," *Metals*, vol. 9, no. 10, pp. 1-11, 2019. [[CrossRef](#)] [[Google Scholar](#)] [[Publisher Link](#)]
- [25] Hua Rong Xin, and Lin Zhu, "Contact Stress FEM Analysis of Deep Groove Ball Bearing Based on ANSYS Workbench," *Applied Mechanics and Materials*, vol. 574, pp. 21-26, 2014. [[CrossRef](#)] [[Google Scholar](#)] [[Publisher Link](#)]
- [26] Anders Flodin, and Soren Andersson, "A Simplified Model for Wear Prediction in Rolling Contacts," *Wear*, vol. 249, no. 3-4, pp. 285-292, 2001. [[CrossRef](#)] [[Google Scholar](#)] [[Publisher Link](#)]
- [27] Mostafa El Laithy et al., "Further Understanding of Rolling Contact Fatigue in Rolling Element Bearings: A Review," *Tribology International*, vol. 140, 2019. [[CrossRef](#)] [[Google Scholar](#)] [[Publisher Link](#)]
- [28] Yu Zhang et al., "Fatigue Life Analysis of Ball Bearings and a Shaft System Considering the Combined Bearing Preload and Angular Misalignment," *Applied Sciences*, vol. 10, no. 8, pp. 1-21, 2020. [[CrossRef](#)] [[Google Scholar](#)] [[Publisher Link](#)]